

Preparation and electrical properties of $\text{Bi}_2\text{Zn}_{2/3}\text{Nb}_{4/3}\text{O}_7$ thin films deposited at room temperature for embedded capacitor applications

Xiaohua Zhang^{a,b}, Wei Ren^{a,b,*}, Peng Shi^{a,b}, M. Saeed Khan^{a,b},
Xiaofeng Chen^{a,b}, Xiaoqing Wu^{a,b}, Xi Yao^{a,b}

^a Electronic Materials Research Laboratory, Key Laboratory of the Ministry of Education, Xi'an Jiaotong University, Xi'an 710049, China

^b International Center for Dielectric Research, Xi'an Jiaotong University, Xi'an 710049, China

Available online 30 April 2011

Abstract

$\text{Bi}_2\text{Zn}_{2/3}\text{Nb}_{4/3}\text{O}_7$ thin films were deposited at room temperature on Pt/Ti/SiO₂/Si(1 0 0) and polymer-based copper clad laminate (CCL) substrates by pulsed laser deposition. $\text{Bi}_2\text{Zn}_{2/3}\text{Nb}_{4/3}\text{O}_7$ thin films were deposited *in situ* with no intentional heating under an oxygen pressure of 4 Pa and then post-annealed at 150 °C for 20 min. It was found that the films are still amorphous in nature, which was confirmed by the XRD analysis. It has been shown that the surface roughness of the substrates has a significant influence on the electrical properties of the dielectric films, especially on the leakage current. $\text{Bi}_2\text{Zn}_{2/3}\text{Nb}_{4/3}\text{O}_7$ thin films deposited on Pt/Ti/SiO₂/Si(1 0 0) substrates exhibit superior dielectric characteristics. The dielectric constant and loss tangent are 59.8 and 0.008 at 10 kHz, respectively. Leakage current density is 2.5×10^{-7} A/cm² at an applied electric field of 400 kV/cm. $\text{Bi}_2\text{Zn}_{2/3}\text{Nb}_{4/3}\text{O}_7$ thin films deposited on CCL substrates exhibit the dielectric constant of 60 and loss tangent of 0.018, respectively. Leakage current density is less than 1×10^{-6} A/cm² at 200 kV/cm.

© 2011 Elsevier Ltd and Techna Group S.r.l. All rights reserved.

Keywords: A. Films; C. Dielectric properties; E. Capacitors; Monoclinic zirconolite

1. Introduction

With the rapid development of microsystems, the compact packages of electronic components have attracted attentions due to their excellent performances [1–3]. The embedded devices can replace the surface mount components, and can considerably reduce the consumed area of printed circuit boards (PCBs) [1]. Embedding passive components into the PCBs is one of the challenging technologies for system miniaturization, good stability, and minimizing parasitic noises [2–5]. The passive components include capacitors, resistors and inductors. Among these components, capacitors are very important in terms of number and size. But it is most difficult to embed capacitors into the PCBs, because of the complicated metal–insulator–metal (MIM) sandwich structures and their unsuitable application sizes can generate the undesired practical

properties [1,3]. The polymer of PCBs cannot accept the processing temperature greater than 200 °C, which restricts the application of high-*k* ferroelectric thin films because of their high processing temperature. Conventional paraelectric materials such as SiO₂ (*k* = 3.9), Ta₂O₅ (*k* = 21–25), and Al₂O₃ (*k* = 8) cannot satisfy the need of embedded capacitors due to their low capacitance densities for the same thickness [1,3,5].

Cubic $\text{Bi}_{1.5}\text{Zn}_{1.0}\text{Nb}_{1.5}\text{O}_7$ (*c*-BZN) and $\text{Bi}_2\text{Mg}_{2/3}\text{Nb}_{4/3}\text{O}_7$ (BMN) pyrochlore materials have been investigated as the dielectrics for the embedded capacitors processed at PCB compatible processing temperatures [6–9]. These thin films fabricated at low temperature exhibit non-crystalline structure and their dielectric constant is approximately in the range of 40–70 [1,5,9]. Monoclinic $\text{Bi}_2\text{Zn}_{2/3}\text{Nb}_{4/3}\text{O}_7$ material possesses a zirconolite structure [6]. The monoclinic $\text{Bi}_2\text{Zn}_{2/3}\text{Nb}_{4/3}\text{O}_7$ ceramics have low-temperature sintering character and exhibit the excellent dielectric properties and high quality factor in the microwave range [10]. The crystalline $\text{Bi}_2\text{Zn}_{2/3}\text{Nb}_{4/3}\text{O}_7$ thin films were also synthesized by the metalorganic deposition process, which exhibit a dielectric constant of 80 and a loss tangent of 0.004 [6]. The temperature capacitance coefficient (TCC) is 150 ppm/°C, which is smaller than that of *c*-BZN thin

* Corresponding author at: Electronic Materials Research Laboratory, Key Laboratory of the Ministry of Education, Xi'an Jiaotong University, Xi'an 710049, China. Tel.: +86 29 82666873; fax: +86 29 82668794.

E-mail address: wren@mail.xjtu.edu.cn (W. Ren).

films (-400 ppm/ $^{\circ}\text{C}$). $\text{Bi}_2\text{Zn}_{2/3}\text{Nb}_{4/3}\text{O}_7$ may be a promising candidate for the embedded capacitor applications.

In this paper, $\text{Bi}_2\text{Zn}_{2/3}\text{Nb}_{4/3}\text{O}_7$ thin films have been prepared on Pt/Ti/SiO₂/Si(1 0 0) and polymer-based copper clad laminate (CCL) substrates by pulsed laser deposition (PLD) process at room temperature. The deposited thin films were post-annealed at 150 $^{\circ}\text{C}$ in air. The structures, dielectric properties and leakage current characteristics of $\text{Bi}_2\text{Zn}_{2/3}\text{Nb}_{4/3}\text{O}_7$ thin films have been investigated.

2. Experimental

The monoclinic zirconolite $\text{Bi}_2\text{Zn}_{2/3}\text{Nb}_{4/3}\text{O}_7$ ceramic targets were prepared by a conventional solid-state reaction process, using raw materials Bi_2O_3 ($>99\%$), ZnO ($>99\%$), and Nb_2O_5 ($>99\%$). The ceramic disks were sintered at 960 $^{\circ}\text{C}$ for 4 h. $\text{Bi}_2\text{Zn}_{2/3}\text{Nb}_{4/3}\text{O}_7$ thin films were directly deposited on Pt/Ti/SiO₂/Si(1 0 0) and polymer-based copper clad laminate (CCL) substrates by a PLD process using a KrF excimer laser (COMPex Pro 205, Coherent Lambda Physik) at a wavelength of 248 nm with a pulse frequency of 3 Hz and pulse width of 30 ns. The depositions were carried out at room temperature with an oxygen pressure of 4 Pa for 60 min. $\text{Bi}_2\text{Zn}_{2/3}\text{Nb}_{4/3}\text{O}_7$ thin films were post-annealed in a rapid thermal process furnace at 150 $^{\circ}\text{C}$ in air for 20 min.

The phase structures were studied by an X-ray diffractometer equipped with Cu K α radiation (XRD, D/Max-2400, Rigaku). Surface morphologies were characterized by an atomic force microscope (AFM, Nanoscope, Veeco) and a scanning electron microscope (SEM, JSM-7000F, JEOL). Thickness of the films was measured by a stylus profiler (Dektak 6M, Veeco). For measuring electrical properties, Au top electrodes with a diameter of 0.5 mm were deposited using DC sputtering via a shadow mask to form a metal–insulator–metal (MIM) structure. The dielectric properties were investigated by using a precision impedance analyzer (4294A, Agilent). Current voltage (I – V) characteristics were examined using a semiconductor characterization system (4200-SCS, Keithley).

3. Results and discussion

Fig. 1 shows the XRD patterns of the $\text{Bi}_2\text{Zn}_{2/3}\text{Nb}_{4/3}\text{O}_7$ ceramic target and thin films deposited on different substrates. The thin films were fabricated under an oxygen pressure of 4 Pa and annealed at 150 $^{\circ}\text{C}$. The main peak of the (2 2 0) plane can be indexed at $2\theta = 29^{\circ}$ for the crystallized $\text{Bi}_2\text{Zn}_{2/3}\text{Nb}_{4/3}\text{O}_7$ ceramic target, as seen in the XRD pattern. By comparing the XRD patterns of the ceramic target and the thin films, it can be found that the thin films show weak and broad peaks at $2\theta = 29^{\circ}$. No other peaks of the zirconolite phase are observed except the peaks of Si wafer and Au, Pt or Cu electrodes. The broad peak around $2\theta = 29^{\circ}$ in the films is related with (2 2 0) peak. It suggests that the nano-sized crystallites may exist in the $\text{Bi}_2\text{Zn}_{2/3}\text{Nb}_{4/3}\text{O}_7$ films except the amorphous states, which were confirmed by the analysis of TEM in the Bi-based pyrochlore films fabricated at low temperature [7,11]. According to the full

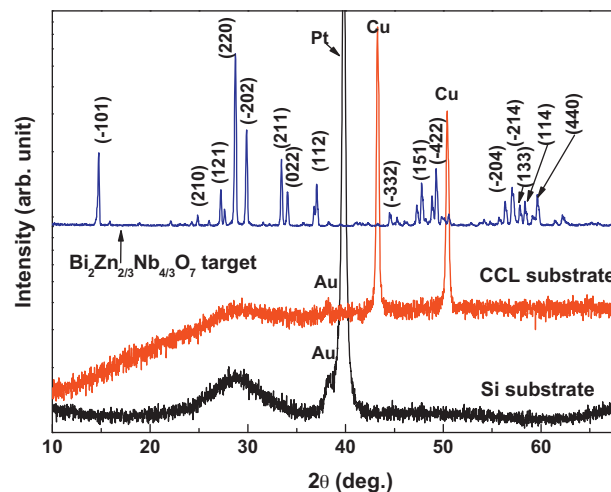


Fig. 1. XRD patterns of $\text{Bi}_2\text{Zn}_{2/3}\text{Nb}_{4/3}\text{O}_7$ ceramic target and thin films deposited on different substrates.

width at half maximum (FWHM) of the broad (2 2 0) peak, the size of crystallites can be estimated using the Scherrer's formula and the average size is approximately 4.5 nm. There is not any obvious difference in the size of crystallites between the films deposited on Si and CCL.

Fig. 2(a) and (b) show the SEM surface and cross-sectional images of the $\text{Bi}_2\text{Zn}_{2/3}\text{Nb}_{4/3}\text{O}_7$ thin film deposited on Pt/Ti/SiO₂/Si(1 0 0). Fig. 2(c) and (d) show the AFM surface and three-dimensional images of the thin film deposited on the CCL substrate. As seen in Fig. 2(a), $\text{Bi}_2\text{Zn}_{2/3}\text{Nb}_{4/3}\text{O}_7$ thin film deposited on Pt/Ti/SiO₂/Si(1 0 0) substrate shows a dense, crack-free surface and the granules are very uniform. Certainly, there are some spherical particles on the surface of the thin film, which are inevitable due to the character of the film deposited by PLD. The cross-sectional image of $\text{Bi}_2\text{Zn}_{2/3}\text{Nb}_{4/3}\text{O}_7$ thin film in Fig. 2(b) also clearly shows a dense structure. The polymer-based CCL substrate was made by preparing the electroless copper on rough polymer substrate. The CCL substrate was characterized using AFM. The root mean square (RMS) value of the surface roughness is approximately 20 nm, which is much larger than that of the platinized silicon substrate (about 2.4 nm). Fig. 2(c) and (d) show a $10\text{ }\mu\text{m} \times 10\text{ }\mu\text{m}$ sized surface image and three-dimensional image of the thin film directly deposited on CCL substrate. It can be seen that the surface of $\text{Bi}_2\text{Zn}_{2/3}\text{Nb}_{4/3}\text{O}_7$ thin film deposited on the rough CCL substrate is also rougher than that of the film deposited on Si substrate. According to the AFM images, the values of the RMS roughness of the thin films on platinized Si and CCL are 3.5 and 21 nm, respectively.

The dielectric properties of $\text{Bi}_2\text{Zn}_{2/3}\text{Nb}_{4/3}\text{O}_7$ thin films deposited on different substrates as a function of measuring frequency are shown in Fig. 3. The measured frequency is in a range of 1 kHz to 1 MHz. The film deposited on Si substrate exhibits an excellent frequency response and the dielectric constant shows little variation with frequency. But for the film deposited on the polymer-based CCL substrate, the dielectric constant decreases with increasing frequency, which attributes to the rough surface of the CCL substrate. The dielectric

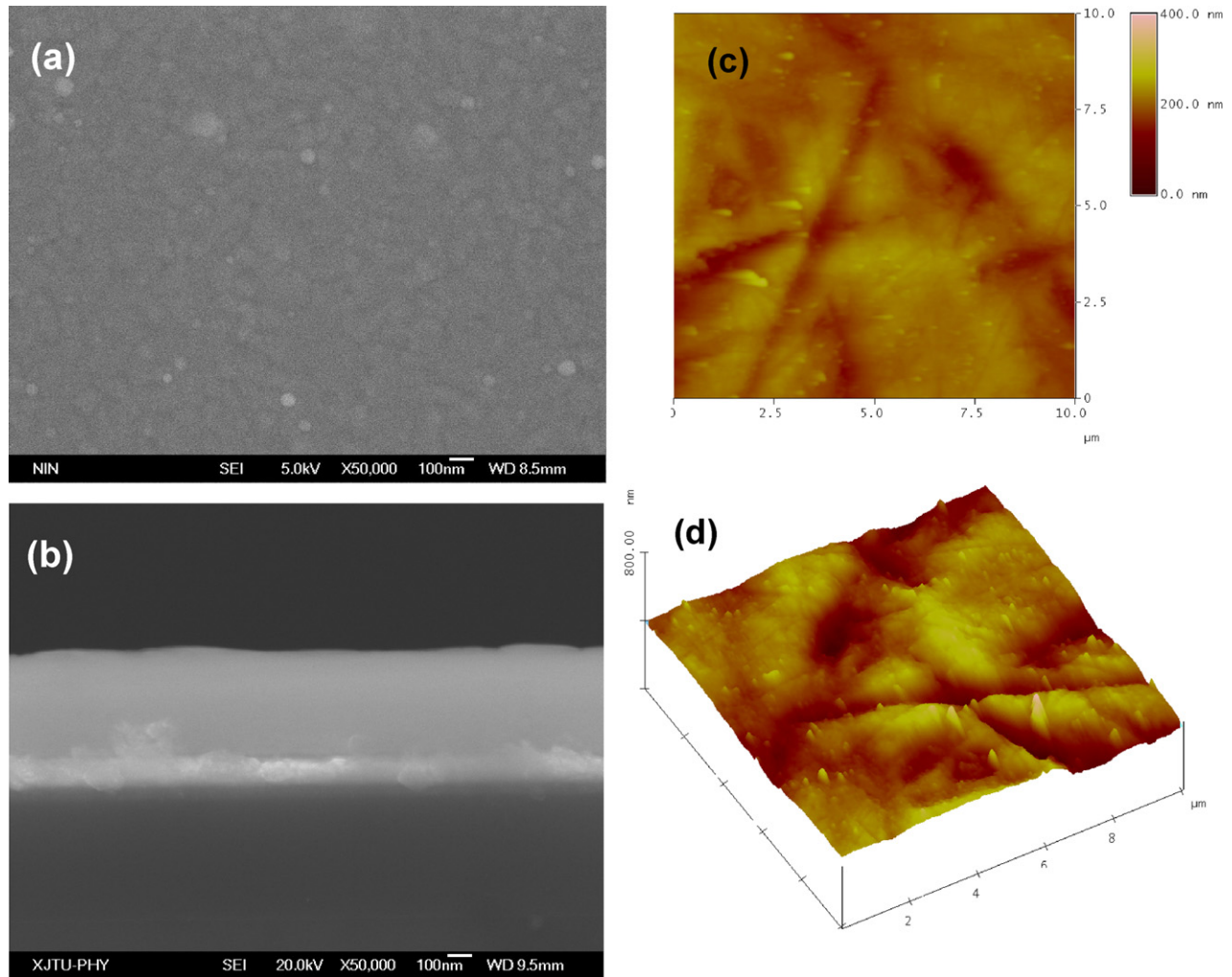


Fig. 2. (a) Surface and (b) cross-sectional SEM images of $\text{Bi}_2\text{Zn}_{2/3}\text{Nb}_{4/3}\text{O}_7$ thin film deposited on Si substrate. (c) AFM surface and (d) three-dimensional images of $\text{Bi}_2\text{Zn}_{2/3}\text{Nb}_{4/3}\text{O}_7$ thin film deposited on polymer-based CCL substrate.

constants of the thin films on both substrates are similar (about 60). However, the loss tangent of the film on CCL is larger than that of the film on Si substrate. The loss tangents of the thin films deposited on Si and CCL substrates are 0.006 and 0.018 at 10 kHz, respectively. The above results suggest that the structures and dielectric properties of $\text{Bi}_2\text{Zn}_{2/3}\text{Nb}_{4/3}\text{O}_7$ thin

films are significantly influenced by the surface roughness of the substrates.

The dielectric constant and loss tangent of $\text{Bi}_2\text{Zn}_{2/3}\text{Nb}_{4/3}\text{O}_7$ thin films as a function of applied voltage are shown in Fig. 4. The measuring frequency is 10 kHz. The dielectric constants show little variation with the applied dc bias field.

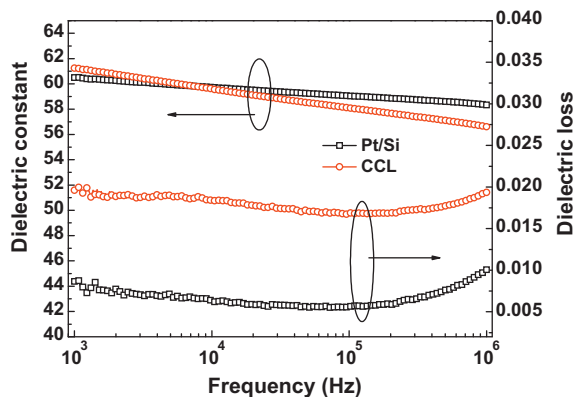


Fig. 3. Frequency dependence of dielectric constant and loss tangent of $\text{Bi}_2\text{Zn}_{2/3}\text{Nb}_{4/3}\text{O}_7$ thin films deposited on different substrates.

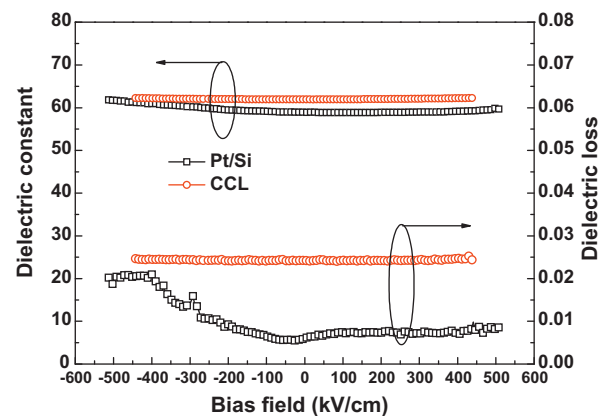


Fig. 4. Dielectric constant and loss tangent at 10 kHz of $\text{Bi}_2\text{Zn}_{2/3}\text{Nb}_{4/3}\text{O}_7$ thin films as a function of applied dc bias field.

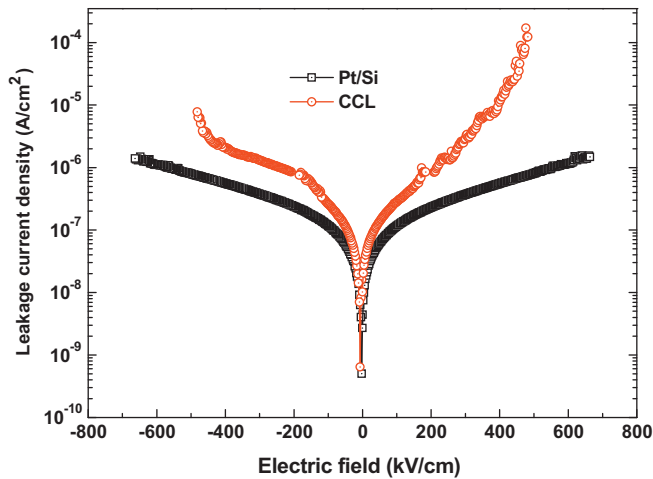


Fig. 5. Leakage current characteristics of $\text{Bi}_2\text{Zn}_{2/3}\text{Nb}_{4/3}\text{O}_7$ thin films deposited on different substrates.

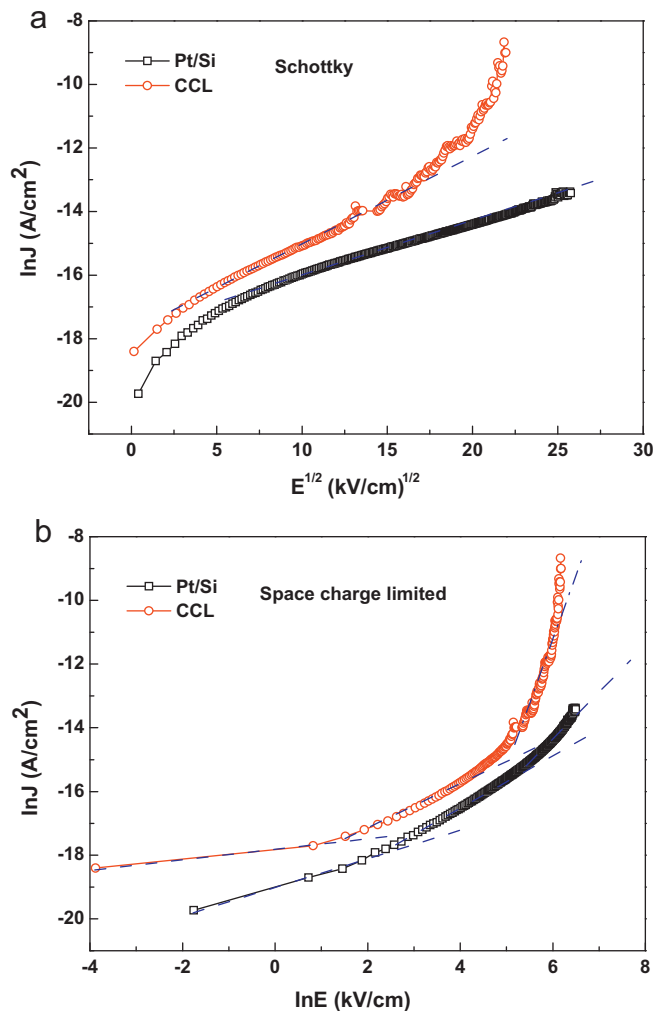


Fig. 6. I – V curves of $\text{Bi}_2\text{Zn}_{2/3}\text{Nb}_{4/3}\text{O}_7$ thin films: (a) $\ln(J)$ versus $E^{1/2}$ and (b) $\ln(J)$ versus $\ln(E)$.

Fig. 5 shows the I – V characteristics of $\text{Bi}_2\text{Zn}_{2/3}\text{Nb}_{4/3}\text{O}_7$ thin films deposited on different substrates as a function of applied bias field. As shown in Fig. 5, the film deposited on Si substrate exhibits lower leakage current density than that of the film deposited on CCL substrate. Like the dielectric properties, the surface roughness of the substrate also plays an important role on the leakage current characteristics. The surface roughness alters the average electrostatic field, resulting in the change of the leakage current of an insulating film [12]. In the parallel-plate capacitor using CCL substrate, the local electric field of the thin film will vary from place to place. The leakage current density is proportional to the exponent of the electric field [12]. In general, the leakage current mechanisms can be attributed to four conduction mechanisms, which are the Schottky emission (Schottky), the Poole–Frenkel (PF) emission, the space-charge-limited current (SCLC) and the Fowler–Nordheim (FN) tunneling behavior [13,14]. To identify the conduction mechanisms in the amorphous $\text{Bi}_2\text{Zn}_{2/3}\text{Nb}_{4/3}\text{O}_7$ films, $\ln(J)$ versus $E^{1/2}$ and $\ln(J)$ versus $\ln(E)$ are plotted according to the Schottky emission mechanism and the space-charge-limited current mechanism in Fig. 6(a) and (b), respectively. The Schottky emission is an interface controlled process. For the films deposited on CCL substrate, it is observed that the curve of the Schottky emission shows good linearity at low electric field. However, the film deposited on Pt/Ti/SiO₂/Si(1 0 0) substrate shows good linearity in the whole electric field range. In addition, the asymmetry of positive and negative leakage currents at the high electric field in Fig. 5 also indicates that the Schottky emission is presented in the amorphous $\text{Bi}_2\text{Zn}_{2/3}\text{Nb}_{4/3}\text{O}_7$ thin films [15]. At the same time, the plots of $\ln(J)$ versus $\ln(E)$ are fitted well by several linear segments with different slopes, as shown in Fig. 6(b), which indicates that the space-charge-limited current mechanism dominates in the thin films [13,14]. Hence, there are two kinds of the conduction mechanisms which are the Schottky emission and the space-charge-limited current, are presented in the $\text{Bi}_2\text{Zn}_{2/3}\text{Nb}_{4/3}\text{O}_7$ films.

4. Conclusions

$\text{Bi}_2\text{Zn}_{2/3}\text{Nb}_{4/3}\text{O}_7$ thin films were prepared on Pt/Ti/SiO₂/Si(1 0 0) and polymer-based copper clad laminate (CCL) substrates by pulsed laser deposition process at room temperature. The thin films deposited on different substrates exhibit similar dielectric constant around 60. However, the surface roughness of the substrates has a significant influence on the dielectric loss and the leakage current, which attributes to the variation of local electric field. The loss tangents of the thin films deposited on Si and CCL substrates are 0.006 and 0.018 at 10 kHz, respectively. Moreover, leakage current densities of the thin films deposited on both substrates are $2.5 \times 10^{-7} \text{ A/cm}^2$ at 400 kV/cm and $1 \times 10^{-6} \text{ A/cm}^2$ at 200 kV/cm, respectively.

Acknowledgements

This work is supported by the National Natural Science Foundation of China (Grant nos. 90923001 and U0634006), by

the International Collaboration Program of the Ministry of Science and Technology of China (Grant no. S2011ZR0272), and by the Shaanxi Province International Collaboration Program (Grant nos. 2009KW-12 and 2010KW-09).

References

- [1] J.H. Park, W.S. Lee, N.J. Seong, S.G. Yoon, S.H. Son, H.M. Chung, J.S. Moon, H.J. Jin, S.E. Lee, J.W. Lee, H.-D. Kang, Y.K. Chung, Y.S. Oh, Bismuth–zinc–niobate embedded capacitors grown at room temperature for printed circuit board applications, *Applied Physics Letters* 88 (2006) 192902.
- [2] J.K. Ahn, H.W. Kim, K.C. Ahn, S.G. Yoon, et al., Characteristics of bismuth-based thin films deposited directly on polymer substrates for embedded capacitor application, *Integrated Ferroelectrics* 95 (2007) 187–195.
- [3] S.E. Lee, J.W. Lee, I.H. Lee, Y.K. Chung, Dielectric properties of PCB embedded bismuth–zinc–niobium films prepared using RF magnetron sputtering, *Materials Research Society Symposium Proceedings* 969 (2007) w01–W07.
- [4] F.E. Kamel, P. Gonon, F. Jomni, Electrical properties of low temperature deposited amorphous barium titanate thin films as dielectrics for integrated capacitors, *Thin Solid Films* 504 (2006) 201–204.
- [5] I.D. Kim, M.H. Lim, K.T. Kang, H.G. Kim, Room temperature fabricated ZnO thin film transistor using high-K $\text{Bi}_{1.5}\text{Zn}_{1.0}\text{Nb}_{1.5}\text{O}_7$ gate insulator prepared by sputtering, *Applied Physics Letters* 89 (2006) 022905.
- [6] W. Ren, S. Trolier-McKinsky, C.A. Randall, T.S. Shrout, Bismuth zinc niobate pyrochlore dielectric thin films for capacitive applications, *Journal of Applied Physics* 89 (2001) 767–774.
- [7] J.H. Park, C.J. Xian, K.C. Ahn, E.T. Kim, S.G. Yoon, J.W. Lee, I.H. Lee, S.E. Lee, B.I. Song, Y.K. Chung, M.K. Jeon, Improvement of leakage current characteristics by plasma treatment in $\text{Bi}_2\text{Mg}_{2/3}\text{Nb}_{4/3}\text{O}_7$ dielectric thin films, *Electrochemical and Solid-State Letters* 10 (2007) G18–G20.
- [8] X.H. Zhang, W. Ren, P. Shi, A.F. Tian, X.F. Chen, X.Q. Wu, X. Yao, Structures and properties of doped bismuth zinc niobate cubic pyrochlore thin films prepared by pulsed laser deposition, *Ferroelectrics* 381 (2009) 87–91.
- [9] J.H. Park, C.J. Xian, N.J. Seong, S.G. Yoon, S.H. Son, H.M. Chung, J.S. Moon, H.J. Jin, S.E. Lee, J.W. Lee, H.D. Kang, Y.K. Chung, Y.S. Oh, Realization of a high capacitance density in $\text{Bi}_2\text{Mg}_{2/3}\text{Nb}_{4/3}\text{O}_7$ pyrochlore thin films deposited directly on polymer substrates for embedded capacitor applications, *Applied Physics Letters* 89 (2006) 232910.
- [10] X.L. Wang, H. Wang, X. Yao, Structures, phase transformations, and dielectric properties of pyrochlores containing bismuth, *Journal of the American Ceramic Society* 80 (1997) 2745–2748.
- [11] C.J. Xian, J.H. Park, K.C. Ahn, S.G. Yoon, J.W. Lee, W.C. Kim, S.T. Lim, S.H. Sohn, J.S. Moon, H.M. Jung, S.E. Lee, I.H. Lee, Y.K. Chung, M.K. Jeon, S.I. Woo, Electrical properties of $\text{Bi}_2\text{Mg}_{2/3}\text{Nb}_{4/3}\text{O}_7$ (BMN) pyrochlore thin films deposited on Pt and Cu metal at low temperatures for embedded capacitor applications, *Applied Physics Letters* 90 (2007) 052903.
- [12] Y.P. Zhao, G.C. Wang, T.M. Lu, G. Palasantzas, J.Th.M. De Hosson, Surface-roughness effect on capacitance and leakage current of an insulating film, *Physical Review B* 60 (1999) 9157–9164.
- [13] X.H. Zhang, W. Ren, P. Shi, X.F. Chen, X.Q. Wu, Effect of oxygen pressure on structure and properties of $\text{Bi}_{1.5}\text{Zn}_{1.0}\text{Nb}_{1.5}\text{O}_7$ pyrochlore thin films prepared by PLD, *Applied Surface Science* 256 (2010) 1861–1865.
- [14] X.H. Zhang, W. Ren, P. Shi, A.F. Tian, H. Xin, X.F. Chen, X.Q. Wu, X. Yao, Influence of substrate temperature on structures and dielectric properties of pyrochlore BZN thin films prepared by pulsed laser deposition, *Applied Surface Science* 256 (2010) 6607–6611.
- [15] N.J. Seong, J.H. Park, S.G. Yoon, Effect of excess bismuth concentration on dielectric and electrical properties of fully crystallized $\text{Bi}_2\text{Mg}_{2/3}\text{Nb}_{4/3}\text{O}_7$ thin films, *Applied Physics Letters* 91 (2007) 072904.